Article

Ion Dynamics and Water Percolation Effects in DNA Polymorphism

Ivan Brovchenko, Aliaksei Krukau, Alla Oleinikova, and Alexey K. Mazur

J. Am. Chem. Soc., **2008**, 130 (1), 121-131 • DOI: 10.1021/ja0732882

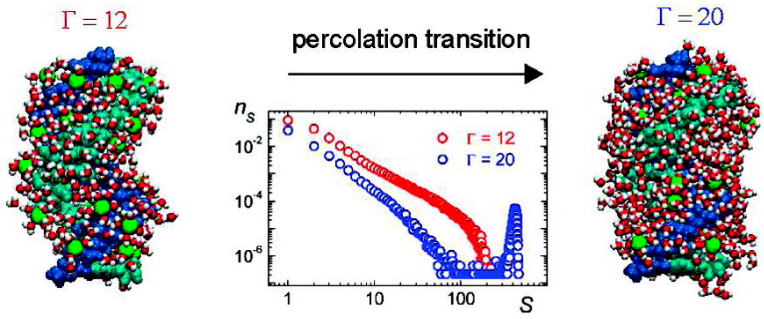

More About This Article

Additional resources and features associated with this article are available within the HTML version:

- Supporting Information
- Links to the 2 articles that cite this article, as of the time of this article download
- Access to high resolution figures
- Links to articles and content related to this article
- Copyright permission to reproduce figures and/or text from this article

View the Full Text HTML

J|A|C|S
ARTICLES
Published on Web 12/06/2007

Ion Dynamics and Water Percolation Effects in DNA Polymorphism

Ivan Brovchenko,[†] Aliaksei Krukau,[†] Alla Oleinikova,[†] and Alexey K. Mazur*[,‡]

Physical Chemistry, Technical University of Dortmund, Otto-Hahn-Str. 6, Dortmund, D-44227, Germany, and CNRS UPR9080, Institut de Biologie Physico-Chimique, 13, rue Pierre et Marie Curie, Paris,75005, France

Received May 9, 2007; E-mail: alexey@ibpc.fr

Abstract: The dynamics of ions and water at the surface of DNA are studied by computer simulations in a wide range of hydrations involving the zone of low-hydration polymorphism in DNA. The long-range mobility of ions exhibits a stepwise increase at three distinct hydration levels. The first of them is close to the midpoint of the water percolation transition as well as the midpoint of the transition between A- and B-DNA forms. It coincides with the onset of the dissociation of ion pairs on the DNA surface probably caused by the increase in the water dielectric permittivity due to the appearance of the spanning hydrogen-bonding network. The other two steps are attributed to the formation of percolating water layers on the surface of DNA accompanied by the progressive escape of ions from the DNA surface. The results agree with earlier experimental data and further corroborate the suggested universal mechanism of the low hydration polymorphism in DNA including intraduplex electrostatic condensation close to the water percolation threshold.

1. Introduction

The double helical DNA may adopt a number of different structural forms.[1] The B-form is the dominant biological conformation while other forms probably exist *in vivo* as high energy states adopted temporarily as shown for A- and Z-DNA.[2−4] The A-form has the same handedness, topology, and hydrogen bonding as the B-form. Its conformation is compatible with any base pair sequence, and its energy is only slightly higher than that of the B-form.[5] Due to all these features, reversible local B ↔ A transitions represent one of the modes for governing protein−DNA interactions.[6] The B ↔ A transitions can be also induced *in vitro* by changing the DNA environment.[7−10] In condensed preparations, that is, in crystalline and amorphous fibers as well as in films, DNA adopts the B-form under high relative humidity, but it can be reversibly driven to the A-form by placing the samples under relative humidity below 80%.[7,9,10] In aqueous solutions single DNA molecules exhibit reversible B ↔ A transitions when certain organic solvents are added.[2,8] In both cases the transition occurs at about the same water activity suggesting that the B ↔ A conformational switch is driven by the hydration state of the double helix.[11] The mechanism and the driving forces of this phenomenon are very controversial.[12−16] A new view emerging in recent years attributes the key role to free metal ions that accumulate in the major groove of B-DNA and, with reduced hydration, provoke intraduplex electrostatic condensation.[17−22] A better understanding of the driving forces of the *in vitro* B ↔ A transition is essential for interpretation of its biological manifestations.

Although the important role of hydration water in DNA conformational stability was always understood and actively investigated, the *spanning* property of the hydrogen bonded (HB) water network on the DNA surface and the possible consequences of its breaking under low hydration only recently attracted attention.[21,22] It is long known that the first monolayer of hydration water is crucial for the activity of biomacromolecules.[23,24] The spanning property of HB water networks first

[†] Technical University of Dortmund.
[‡] Institut de Biologie Physico-Chimique.

(1) Saenger, W. *Principles of Nucleic Acid Structure*; Springer-Verlag: New York, 1984.
(2) Ivanov, V. I.; Minchenkova, L. E. *Mol. Biol.* **1995**, *28*, 780−788.
(3) Lu, X. J.; Shakked, Z.; Olson, W. K. *J. Mol. Biol.* **2000**, *300*, 819−840.
(4) Rich, A.; Zhang, S. *Nat. Rev. Genet.* **2003**, *4*, 566−72.
(5) Tolstorukov, M. Y.; Ivanov, V. I.; Malenkov, G. G.; Jernigan, R. L.; Zhurkin, V. B. *Biophys. J.* **2001**, *81*, 3409−3421.
(6) Ng, H.-L.; Kopka, M. L.; Dickerson, R. E. *Proc. Natl. Acad. Sci. U.S.A.* **2000**, *97*, 2035−2039.
(7) Franklin, R. E.; Gosling, R. G. *Nature* **1953**, *171*, 740−741.
(8) Tunis-Schneider, M. J.; Maestre, M. F. *J. Mol. Biol.* **1970**, 52, 521−541.
(9) Leslie, A. G. W.; Arnott, S.; Chandrasekaran, R.; Ratliff, R. L. *J. Mol. Biol.* **1980**, *143*, 49−72.
(10) Piskur, J.; Rupprecht, A. *FEBS Lett.* **1995**, *375*, 174−178.
(11) Malenkov, G.; Minchenkova, L.; Minyat, E.; Schyolkina, A.; Ivanov, V. *FEBS Lett.* **1975**, *51*, 38−42.
(12) Ivanov, V. I.; Minchenkova, L. E.; Schyolkina, A. K.; Poletaev, A. I. *Biopolymers* **1973**, *12*, 89−110.
(13) Calladine, C. R.; Drew, H. R. *J. Mol. Biol.* **1984**, *178*, 773−782.
(14) Saenger, W.; Hunter, W. N.; Kennard, O. *Nature* **1986**, *324*, 385−388.
(15) Fuller, W.; Mahensdasingam, A.; Forsyth, V. T. *Nature* **1988**, 335, 596.
(16) Hunter, C. A. *J. Mol. Biol.* **1993**, *230*, 1025−1054.
(17) Cheatham, T. E., III; Crowley, M. F.; Fox, T.; Kollman, P. A. *Proc. Natl. Acad. Sci. U.S.A.* **1997**, *94*, 9626−9630.
(18) Cheatham, T. E., III; Kollman, P. A. *Structure* **1997**, *5*, 1297−1311.
(19) Mazur, A. K. *J. Am. Chem. Soc.* **2003**, *125*, 7849−7859.
(20) Mazur, A. K. *J. Chem. Theory Comput.* **2005**, *1*, 325−336.
(21) Brovchenko, I.; Krukau, A.; Oleinikova, A.; Mazur, A. K. *Phys. Rev. Lett.* **2006**, *97*, 137801(4).
(22) Brovchenko, I.; Krukau, A.; Oleinikova, A.; Mazur, A. K. *J. Phys. Chem. B* **2007**, *111*, 3258−3266.
(23) Kuntz, I. D.; Kauzmann, W. *Adv. Protein Chem.* **1974**, *28*, 239−345.
(24) Rupley, J. A.; Careri, G. *Adv. Protein Chem.* **1991**, *41*, 37−172.

discovered two decades ago is particularly important.[25,26] When a small number of water molecules are adsorbed at a hydrophilic surface they are dispersed in a large number of small clusters. At a certain critical hydration these clusters undergo a quasi-2D percolation transition and merge into a single spanning HB network, which usually coincides with rapid recovery of biological activity.[24−30] Efficient theoretical and simulation methods for studying this phenomenon have been developed.[31] A quasi-2D percolation transition in hydrated protein powders was reproduced in molecular dynamics (MD) simulations, with the hydration threshold close to experiment.[32] The hydration shell on finite hydrophilic surfaces is also formed via a quasi-2D percolation transition, with the universal properties of percolation reproduced.[31,33−35] The effect was already observed in a variety of systems, notably, for hydration of a single lysozyme molecule,[32,35] for cooling of SNase and elastin-like peptide in dilute solutions,[36] and for pressurization of a crystalline SNase.[37] The water percolation transition is arguably related to conformational dynamics of hydrated biomolecules;[31,36] however, the microscopic origin of this relationship is unclear. It was suggested that the spanning network of hydration water facilitates the conformational mobility[24] and the charge transport along macromolecular surfaces.[25] Other factors can also be involved, notably, the increase of water density fluctuations at the percolation transition and the increase of water dielectric permittivity upon formation of the spanning HB network. A reasonable approach to this problem consists of studying various properties of hydrated biomolecules when crossing the water percolation threshold.

Hydration of nucleic acids has a number of distinctions due to their polyionic character and uneven nonspherical shapes.[1] Under physiological conditions, the double helical DNA directly interacts with solvent ions at several water layers from its surface; therefore, the functional DNA hydration shell is very thick. Under limited hydration, there is a strict relationship between the state of DNA and the hydration number Γ measured as the number of water molecules per nucleotide (or phosphate). When Γ is reduced below 30, the B-form of DNA is already perturbed, but it is maintained until $\Gamma \approx 20$.[1,9] Below this hydration, DNA undergoes different conformational transitions depending upon its sequence, bound metal ions, and other environmental conditions. The most studied is the transition from the B- to A-form, with the midpoint at about $\Gamma \approx 15$.[1,38,39] Recent simulation studies[21,22] revealed that the breakdown of the spanning water network on the surface of model B- and A-DNA molecules upon dehydration occurs close to the experimental midpoint of the B to A transition. It was found that free ions shift the threshold by hampering H-bonded networking for water molecules of their coordination shells[22] and that their long-range mobility is strongly accelerated in the presence of the spanning water network in good agreement with the experimental DNA conductivity.[21,40] To shed new light on the possible mechanisms of polymorphic transitions that occur in weakly hydrated double helical DNA here we study the interplay of water percolation and ion dynamics in DNA hydration shells in a wide range of hydrations including the midpoint of the transitions between A- and B-forms. It is shown that diffusion of water and ions near DNA exhibits properties typical for confined systems with strong spatial disorder. Analysis of the dependence of the long-range ion mobility upon hydration reveals three states where a stepwise increase in the diffusion rates is observed. The first of them is close to the midpoint of the water percolation transition. It coincides with the onset of the dissociation of ion pairs on the DNA surface caused by the increase in water dielectric permittivity due to the appearance of the spanning HB network. The other two steps are attributed to the formation of percolating water layers on the surface of DNA accompanied by the progressive escape of ions to the environment. The results agree with earlier experimental data and further corroborate the suggested universal mechanism of the low hydration polymorphism in DNA including intraduplex electrostatic condensation close to the water percolation threshold.

2. Methods

MD simulations were carried out for hydration shells of a rigid dodecamer DNA duplex, with the hydration numbers Γ varied around the experimental midpoint of the A ↔ B transition. The double helical DNA fragment with the sequence CGCGAATTCGCG was considered in two alternative conformations corresponding to the canonical A- and B-DNA structures.[41] For better comparison with the previous studies,[17−22] the Cornell et al. force field[42] was used with the TIP3P water[43] and Na^+ parametrization due to Åqvist.[44] The simulation protocols were similar to the earlier water drop calculations[19,20,45] except that the DNA molecule was rigid and fixed in space. The last choice was based upon the following considerations. Earlier calculations showed that in the present conditions the midpoint of the A ↔ B transition is observed at $\Gamma \approx 25$,[19] whereas the corresponding experimental value for random DNA is $\Gamma \approx 15$.[39,40] These two values are remarkably close, and the difference can be attributed to the known small A-philic bias of the present DNA parametrization.[46] For the purposes of the present study, however, this discrepancy is significant. Indeed, according to experiment, with $\Gamma \approx 15$, long double helical DNA should represent a 50% mixture of short stretches of A- and B-forms alternating along the polymer chain. Unlike that, the flexible model of this DNA fragment adopts only an A-form in water drops corresponding to $\Gamma < 20$. In

(25) Gascoyne, P. R.; Pethig, R.; Szent-Gyorgyi, A. *Proc. Natl. Acad. Sci. U.S.A.* **1981**, *78*, 261−265.
(26) Careri, G.; Giansanti, A.; Rupley, J. A. *Proc. Natl. Acad. Sci. U.S.A.* **1986**, *83*, 6810−6814.
(27) Careri, G.; Giansanti, A.; Rupley, J. A. *Phys. Rev. A* **1988**, 37, 2703−2705.
(28) Rupley, J. A.; Siemankowski, L.; Careri, G.; Bruni, F. *Proc. Natl. Acad. Sci. U.S.A.* **1988**, *85*, 9022−9025.
(29) Bruni, F.; Careri, G.; Leopold, A. C. *Phys. Rev. A* **1989**, *40*, 2803−2805.
(30) Bruni, F.; Careri, G.; Clegg, J. S. *Biophys. J.* **1989**, *55*, 331−338.
(31) Oleinikova, A.; Brovchenko, I. *Mol. Phys.* **2006**, *104*, 3841−3855.
(32) Oleinikova, A.; Smolin, N.; Brovchenko, I.; Geiger, A.; Winter, R. *J. Phys. Chem. B* **2005**, *109*, 1988−1998.
(33) Brovchenko, I.; Oleinikova, A. In *Handbook of Theoretical and Computational Nanotechnology*, *Volume 1*; Rieth, M., Schommers, W., Eds.; American Scientific Publishers: Stevenson Ranch, CA, 2006; pp 1−98.
(34) Oleinikova, A.; Brovchenko, I.; Geiger, A. *Physica A* **2006**, *364*, 1−12.
(35) Smolin, N.; Oleinikova, A.; Brovchenko, I.; Geiger, A.; Winter, R. *J. Phys. Chem. B* **2005**, *109*, 10995−11005.
(36) Brovchenko, I.; Krukau, A.; Smolin, N.; Oleinikova, A.; Geiger, A.; Winter, R. *J. Chem. Phys.* **2005**, *123*, 224905.
(37) Oleinikova, A.; Smolin, N.; Brovchenko, I. *J. Phys. Chem. B* **2006**, *110*, 19619−19624.
(38) Texter, J. *Prog. Biophys. Molec. Biol.* **1979**, *33*, 83−97.
(39) van Dam, L.; Korolev, N.; Nordenskiöld, L. *Nucleic Acids Res.* **2002**, *30*, 419−428.
(40) Warman, J. M.; de Haas, M. P.; Rupprecht, A. *Chem. Phys. Lett.* **1996**, *249*, 319−322.
(41) Arnott, S.; Hukins, D. W. L. *Biochem. Biophys. Res. Commun.* **1972**, *47*, 1504−1509.
(42) Cornell, W. D.; Cieplak, P.; Bayly, C. I.; Gould, I. R.; Merz, K. M.; Ferguson, D. M.; Spellmeyer, D. C.; Fox, T.; Caldwell, J. W.; Kollman, P. A. *J. Am. Chem. Soc.* **1995**, *117*, 5179−5197.
(43) Jorgensen, W. L.; Chandreskhar, J.; Madura, J. D.; Impey, R. W.; Klein, M. L. *J. Chem. Phys* **1983**, *79*, 926−935.
(44) Åqvist, J. *J. Phys. Chem.* **1990**, *94*, 8021−8024.
(45) Mazur, A. K. *J. Am. Chem. Soc.* **2002**, *124*, 14707−14715.
(46) Cheatham, T. E., III; Kollman, P. A. *Annu. Rev. Phys. Chem.* **2000**, *51*, 435−471.

these conditions, the fixed canonical A- and B-DNA structures provide a reasonably good approximation of the two states of the contact surface between DNA and water. Earlier studies showed that fixation itself has only a minor effect upon water clustering on the surface of biomacromolecules.[47]

The starting states for Γ from 10 to 30 were prepared as follows. The DNA duplex was first immersed in a large rectangular water box, and the external solvent molecules were removed by using a spherical distance cutoff from DNA atoms. The cutoff radius was adjusted to obtain the desired hydration level. The drop was neutralized by randomly placing 22 Na^+ ions at water positions selected so that their distances from DNA were larger than a small cutoff distance depending on the drop size. No excess salt was added. Our previous simulations revealed that the excess NaCl rapidly forms crystals during water drop simulations with only a minor effect on the A $\leftrightarrow$ B transitions,[19] which agrees with early experimental observations.[48,49] In experiments, the A $\leftrightarrow$ B transitions in DNA are usually studied with possibly low salt concentration to avoid precipitation.[50] For comparative ion-free simulations, the DNA fragment was neutralized by evenly distributing the compensating charge between all DNA atoms.

Atom trajectories were produced by using the water drop method with the long-range electrostatic interactions computed by the Ewald summation algorithm modified for infinite vacuum boundaries.[45] The internal coordinate molecular dynamics (ICMD)[51,52] was used with increased inertia of water molecules[53] and a time step of 0.01 ps. The starting state was energy minimized, and dynamics were initiated with the Maxwell distribution of generalized momenta at low temperature. The system was next slowly heated and equilibrated during 1 ns. The temperature was maintained at 300 K by the Berendsen thermostat[54] with a relaxation time of 10 ps. No restraining potentials were applied to prevent water evaporation. Instead water−solute distances were checked every 150 ps, and distant water molecules were repositioned randomly in close proximity of the hydration shell with zero velocities. On average, the number of such molecules was less than one and their effect was considered insignificant. The standard duration of production runs was 10 ns with the coordinates saved every picosecond. Very similar results were obtained in trial runs of 1 ns with coordinates saved every 100 fs.

The statistical analysis of water and ion diffusion is carried out by averaging over all relevant atom trajectories of a given duration starting at different moments. Because of the natural spatial confinement, the time dependence of the mean-square displacement $\langle r^2 \rangle$ of molecules in a water drop is nonlinear and achieves saturation at long times. Therefore, diffusion properties should be evaluated separately for different time scales. Two measurable parameters are used for that purpose. The mean-square displacement $\langle r_\tau^2 \rangle$ is evaluated for a certain reference duration of diffusion τ. This parameter characterizes the average integral mobility over all shorter periods. In contrast, the time-dependent diffusion coefficient D_τ characterizes the instantaneous rate of diffusion. It is computed by linear regression analysis of an interval 2Δ around the reference duration τ of the $r^2(t)$ plots as

$$D_\tau = \frac{\langle r^2(\tau + \Delta) - r^2(\tau - \Delta) \rangle}{2d\Delta} \quad (1)$$

where d is the Euclidean dimension of the system. We used $\tau = 10$ ps with $\Delta = 5$ ps and $\tau = 75$ ps with $\Delta = 25$ ps for characterizing the short-range mobility of both water and ions. To characterize the long-range mobility, we used $\tau = 200$ ps with $\Delta = 100$ ps for water and $\tau = 350$ ps with $\Delta = 150$ ps. The reference τ and Δ values for the long-range mobility are chosen so that the corresponding mean square displacements were as large as possible, but somewhat smaller than the system size to avoid saturation effects.

The surface radial distribution functions of Na^+ ions were computed by considering only the B-DNA major groove hydration shell where significant qualitative changes are observed with varied hydration.[22] To this end the sugar−phosphate backbone O1P atoms that face one another in the major groove were joined by straight lines, and the set of the corresponding middle points was used as landmarks. Sodium ions within 7.5 Å of these reference points were considered as belonging to the major groove. This procedure is simple and provides a rather good selection due to the fixed regular DNA structure. The Na^+ ions were counted in consecutive 0.1 Å thick layers around DNA by using as a criterion the minimal distance from a given ion to any non-hydrogen DNA atom. The layer volumes were estimated by using the Monte Carlo method.

The clustering and percolation of water were analyzed by methods earlier developed in our group.[32,34−36,55] Water molecules belong to the same cluster if they are connected by a continuous path of hydrogen bonds (H-bonds).[32,56,57] Two water molecules were considered as H-bonded when the distance between the oxygen atoms is < 3.5 Å and the water−water interaction energy is < -2.3 kcal/mol. To locate the percolation threshold of water and to characterize the formation of a spanning water network, various properties of water clusters were calculated for each saved configuration and averaged over 10^4 configurations. The cluster size distribution n_S is the occurrence probability of clusters of size S measured as the number of water molecules in the cluster. The percolation threshold is reached when the cluster size distribution obeys a universal power law $n_S \approx S^{-\tau}$ in the widest range of cluster sizes S, where $\tau = 187/91 \approx 2.05$ in the case of 2D percolation.[58] The corresponding hydration number is denoted as Γ_t. The mean cluster size S_{mean} was calculated as

$$S_{\mathrm{mean}} = \frac{\sum n_S S^2}{\sum n_S S}$$

excluding the largest cluster from the sum. In finite systems, S_{mean} passes through a maximum below the percolation threshold. The probability distribution $P(S_{\mathrm{max}})$ of the size S_{max} of the largest water cluster is used for estimating the spanning probability R, that is the probability to observe a spanning cluster in an arbitrary chosen configuration. Its value is obtained as an integral of $P(S_{\mathrm{max}})$ over $S_{\mathrm{max}} > 0.5N_{\mathrm{w}}$, where $N_{\mathrm{w}} = 24\Gamma$ is the total number of water molecules.[31,34,36] When the system passes through a percolation transition the spanning probability $R(\Gamma)$ shows a sigmoidal dependence with an inflection point at Γ_{m} called the midpoint of the transition. Note that for 2D percolation at the surface of a finite object $\Gamma_{\mathrm{m}} \leq \Gamma_t$.[31]

3. Results

3.1. Water and Ion Mobility. 3.1.1. B-DNA Hydration Shell. Figure 1 exhibits the time dependences of the mean square displacement of water oxygens measured under different hydrations. The observed shape of the $\langle r^2 \rangle(t)$ traces is typical for confined systems.[59] Atom trajectories are naturally limited by

(47) Oleinikova, A.; Smolin, N.; Brovchenko, I. *Biophys. J.* **2007**, *93*, 2986−3000.
(48) Zimmerman, S. B.; Pheiffer, B. H. *J. Mol. Biol.* **1980**, *142*, 315−330.
(49) Cooper, P. J.; Hamilton, L. D. *J. Mol. Biol.* **1966**, *16*, 562−563.
(50) Ivanov, V. I.; Minchenkova, L. E.; Minyat, E. E.; Schyolkina, A. K. *Cold Spring Harbor Symp. Quant. Biol.* **1983**, *47*, 243−250.
(51) Mazur, A. K. *J. Comput. Chem.* **1997**, *18*, 1354−1364.
(52) Mazur, A. K. In *Computational Biochemistry and Biophysics*; Becker, O. M., MacKerell, A. D., Jr., Roux, B., Watanabe, M., Eds.; Marcel Dekker: New York, 2001; pp 115−131.
(53) Mazur, A. K. *J. Phys. Chem. B* **1998**, *102*, 473−479.
(54) Berendsen, H. J. C.; Postma, J. P. M.; van Gunsteren, W. F.; DiNola, A.; Haak, J. R. *J. Chem. Phys.* **1984**, *81*, 3684−3690.
(55) Oleinikova, A.; Brovchenko, I.; Smolin, N.; Krukau, A.; Geiger, A.; Winter, R. *Phys. Rev. Lett.* **2005**, *95*, 247802.
(56) Geiger, A.; Stillinger, F.; Rahman, A. *J. Chem. Phys.* **1979**, 70, 4185−4193.
(57) Oleinikova, A.; Brovchenko, I.; Geiger, A.; Guillot, B. *J. Chem. Phys.* **2002**, *117*, 3296−3304.
(58) Stauffer, D. *Introduction to percolation theory*; Taylor and Francis: London and Philadelphia, 1985.
(59) Brovchenko, I.; Geiger, A.; Oleinikova, A.; Paschek, D. *Eur. Phys. J. E* **2003**, *12*, 69−76.

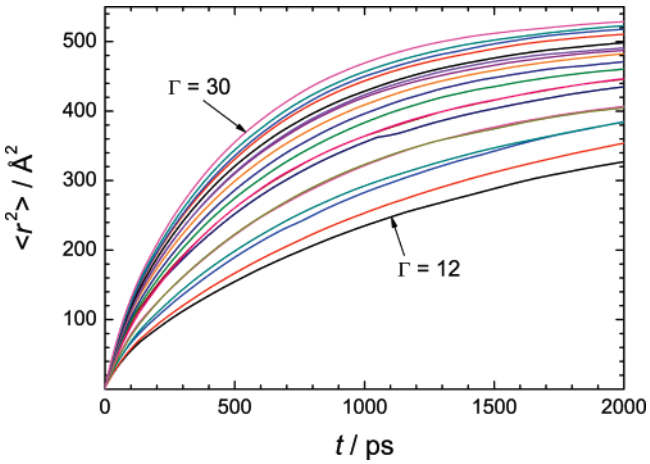

Figure 1. Time dependence of the mean-square displacements $\langle r^2 \rangle$ of water molecules at the surfaces of B-DNA at various hydrations Γ.

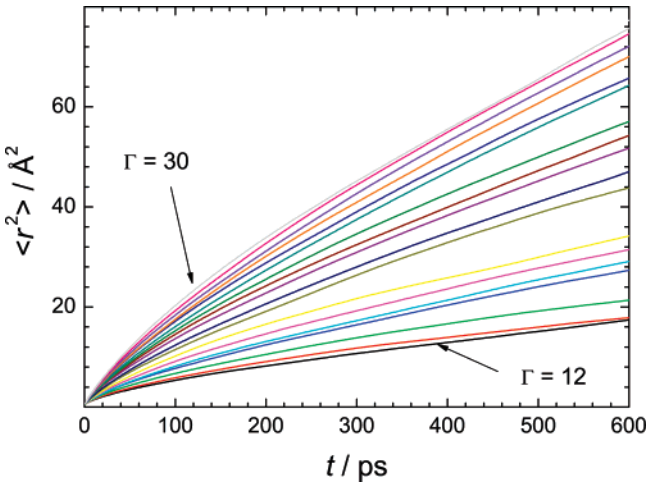

Figure 2. Time dependence of the mean-square displacements $\langle r^2 \rangle$ of ions at the surfaces of B-DNA at various hydrations Γ.

the system size and with $t \rightarrow \infty$ all plots should reach some plateau. This implies that the time dependence of $\langle r^2 \rangle(t)$ can be linear for small t only. Additionally, even for time intervals much smaller than the saturation limit, the nonlinearity in the time dependence of $\langle r^2 \rangle(t)$ can originate from the temporal and/or spatial disorder. This regime, referred to as "anomalous diffusion", is characterized by a power law $\langle r^2 \rangle \approx t^{\alpha}$, with $\alpha < 1$, and it is typical for water diffusion near biosurfaces.[47,60,61] The anomalous diffusion was really observed in our simulations, but it will be analyzed in a separate publication. The saturation of the mean-square displacements of water molecules occurs at distances that grow with the hydration number and reasonably agree with the size of the water drop. Figure 2 exhibits the corresponding time dependences of the mean square displacement of Na^+ ions. The $\langle r^2 \rangle(t)$ traces are qualitatively similar to water plots in Figure 1, with much lower absolute migration rates. Due to this lower mobility, ion displacements become comparable with the size of the drop for much larger time intervals, and plots in Figure 2 feature only the diffusion regime before saturation. The above considerations concerning the anomalous diffusion of water also apply for ions.

Figures 1 and 2 show that the mobilities of water and ions gradually grow with hydration number Γ. It was recently

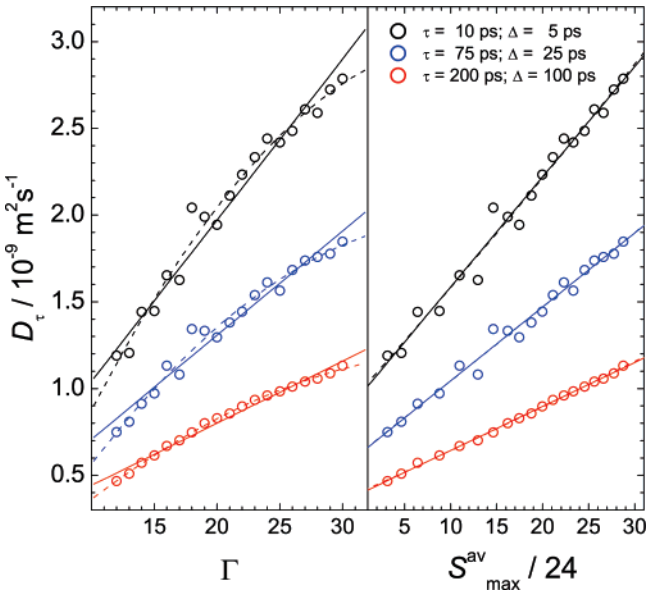

Figure 3. Time dependent diffusion coefficients of water in B-DNA hydration shell as functions of hydration level Γ (left panel) and of the average size S^{av}_{max} of the largest water clusters (right panel). The corresponding values of τ and Δ are shown in the figure. Linear and second-order polynomial fits are shown in both panels by solid and dashed lines, respectively.

shown[21] that for ions this growth is not always steady and that it depends upon the qualitative properties of the HB network of hydration water around DNA. Taking into account the nonlinear time dependence of $\langle r^2 \rangle(t)$ due to the confinement effect and the anomalous character of the diffusion, the quantitative analysis of the corresponding diffusion rates is carried out separately for different time scales by using the mean square displacement $\langle r_\tau^2 \rangle$ and the time dependent diffusion coefficient D_τ with different reference time τ (see Methods). Figure 3 shows that the short-range and the long-range mobilities of water depend upon hydration very similarly. They both increase and display a weak trend to saturation. Strong fluctuations of the short-range mobility rates are seen in the range of Γ from 16 to 20, which is immediately above the percolation threshold observed at $\Gamma_t \approx 15.5$.[21,22] These fluctuations hide the regular trend, but still the points follow a single concave curve suggesting that there are no drastic changes in the mechanisms of water translational diffusion in the range of hydrations studied. An interesting correlation is revealed in the right panel of Figure 3. Here the same data are replotted by using on the X-axis the average size S^{av}_{max} of the maximal water cluster measured as the number of molecules involved. Below the percolation threshold at $\Gamma_t \approx 15.5$, the hydration shell is dispersed in a large number of small clusters and $S^{av}_{max}/24 \ll \Gamma$. In contrast, with $\Gamma > \Gamma_t$ the maximal cluster involves almost all available water molecules and $S^{av}_{max}/24 \rightarrow \Gamma$. Figure 3 shows that there is a good linear correlation between water mobility and S^{av}_{max}. We do not know if there are some physical reasons behind this observation.

The dependence of ion mobility on hydration is analyzed in Figures 4 and 5. The short-range mobility (Figure 4) exhibits nearly linear growth in the whole range of hydrations studied. Comparison of Figures 3 and 4 reveals clear qualitative differences. Indeed, the plots for short-range water mobility in Figure 3 are evidently nonlinear and they also exhibit much

(60) Settles, M.; Doster, W. *Faraday Discuss.* **1996**, *103*, 269−279.
(61) Bizzarri, A. R.; Cannistraro, S. *Phys. Rev. E* **1996**, *53*, R3040−R3043.

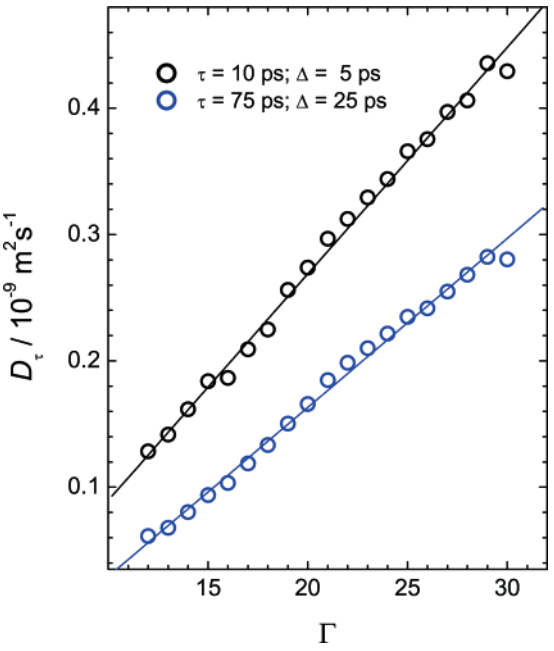

Figure 4. Time dependent diffusion coefficients of ions in B-DNA hydration shell as functions of hydration level Γ. The corresponding values of τ and Δ are shown in the figure. Linear fits are shown by solid lines.

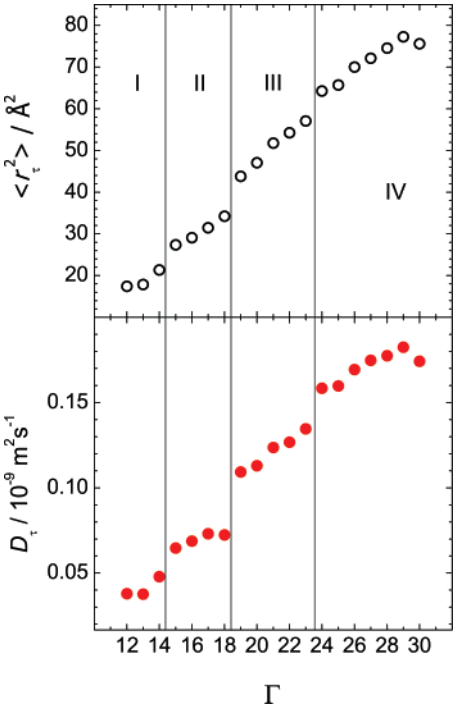

Figure 5. Long-range mobility of ions in B-DNA hydration shell at various hydration levels characterized by mean-square displacement $\langle r^2 \rangle$ at $t = 600$ ps (upper panel) and by the time dependent diffusion coefficient D_τ calculated by eq 1 at $\tau = 350$ ps with $\Delta = 150$ ps. Vertical lines separate the regions with different behaviors of D_τ with hydration Γ.

larger fluctuations. This observation suggests that water and ion translational mobilities are governed by different factors. Note that water and ion motions occur on different length scales. Water molecules that interact with ions represent a small slow moving fraction that makes a negligible contribution in Figure 3. The latter mainly shows water translations in the space free of ions. In contrast, ion dynamics analyzed in Figure 4 involves short moves of 1−2 Å that can occur due to water rotations as

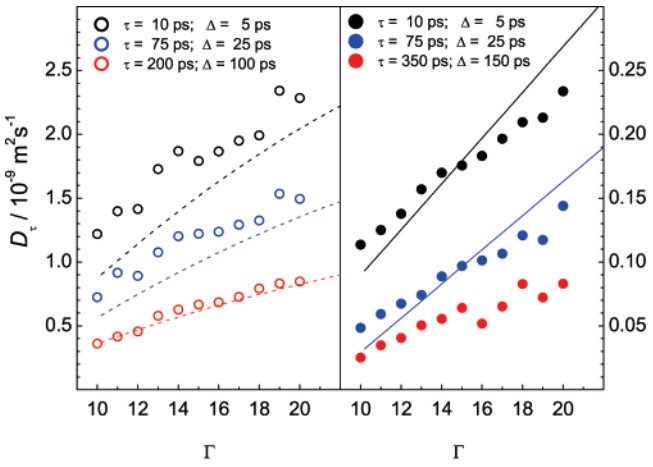

Figure 6. Time dependent diffusion coefficients of water (left pannel) and ions (right pannel) in A-DNA hydration shell as functions of hydration number Γ. The corresponding values of τ and Δ are shown in the figure. The dashed and solid lines display the polynomial fits of the corresponding dependences for B-DNA shown in Figures 3 and 4, respectively.

well as translations. The linear growth of the short-length ion mobility in Figure 4 is not trivial and can be due to a combination of several factors. Under very low hydration, the residual water molecules are strongly bound to ions and charged DNA groups. The rotational dynamics of this water is hindered. According to experiment, "freely" rotating water molecules appear with increased hydration already at relatively low hydrations (at $\Gamma \geq 8$ for Na-DNA), and their number linearly grows with Γ.[62] It is also possible that the ion mobility simply grows with the volume of the accessible space. Additional studies are necessary to clarify these issues.

The long-range ion mobility shown in Figure 5 looks quite different from that shown in Figure 4. On the one hand, evident regular growth is seen that may have the same origin as that in Figure 4. On the other hand, three steps are distinguished where the long-range ion mobility increases drastically suggesting qualitative changes in the diffusion regime. The jumps occur at $\Gamma \approx 14.5$, 18.5, and 23.5, respectively, and they are more pronounced in the $D_\tau(\Gamma)$ trace, which is not surprising since the $\langle r_\tau^2 \rangle(\Gamma)$ plot involves a contribution from the linear short-range regime shown in Figure 4. Figure 5 indicates that the contribution of the long-range diffusion in the integral mobility is dominating. The long-range contribution should grow further with increased DNA length and diffusion distances.

3.1.2. A-DNA Hydration Shell. The mean square displacements of water and ions in A-DNA hydration shells change with time and hydration number similarly to those in Figures 1 and 2 (not shown). Figure 6 confirms that the corresponding diffusion coefficients D_τ steadily grow with Γ on all time scales and in the whole range of hydrations studied. Earlier analysis of water clustering showed that the spanning HB network around A- and B-DNA is formed via a percolation transition with the midpoints at $\Gamma_m \approx 12.9$ and $\Gamma_m \approx 14.3$, respectively, and that the percolation threshold is observed with $\Gamma_t \approx 15.5$ in both cases.[22] Comparison with Figure 6 suggests that the spanning HB water network around A-DNA hinders the growth of $D_\tau(\Gamma)$ for both water and ions. The effect is distinguishable on all time scales in spite of occasional significant noise. Water is more mobile in hydration shells of A-DNA compared to B-DNA. For

(62) Lee, R. S.; Bone, S. *Faraday Discuss.* **1996**, *103*, 59−69.

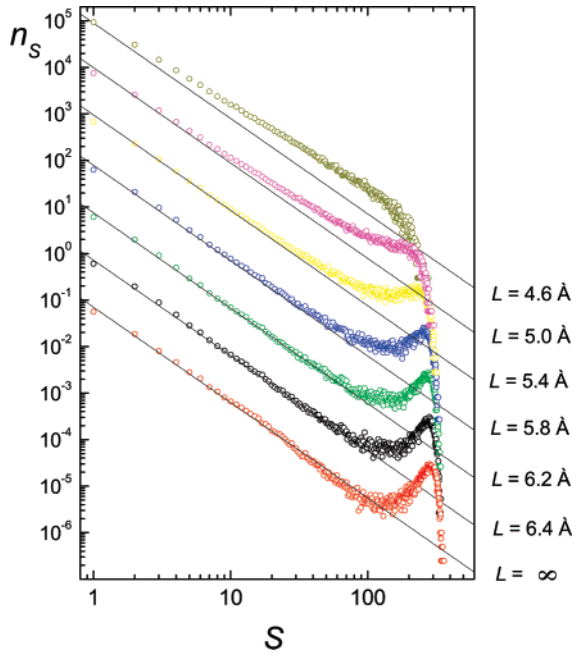

Figure 7. Hydrated DNA with ions. The probability n_S to find a water cluster of size S in layers of different thickness around DNA under hydration $\Gamma = 16$, i.e., close to the percolation threshold $\Gamma_t \approx 15.5$.[21,22] The power law distribution expected at the percolation threshold is shown by straight lines. For clarity, the distributions are shifted consecutively along the Y-axis by 1 order of magnitude each, starting from the bottom.

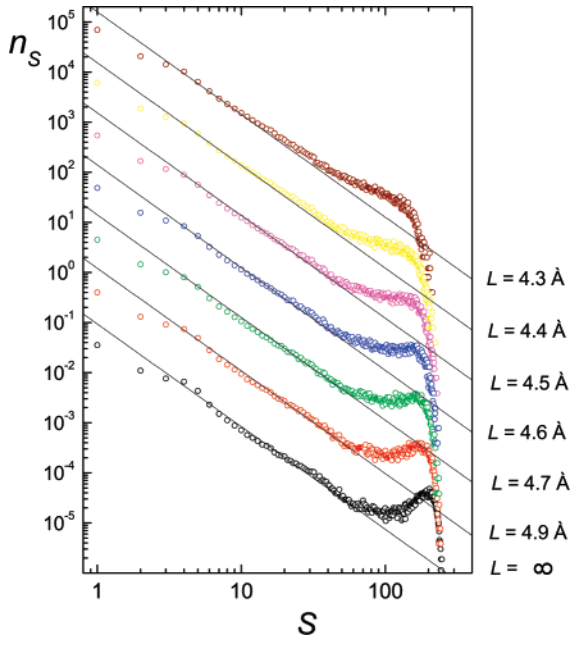

Figure 8. Hydrated DNA without ions. The probability n_S to find a water cluster of size S in layers of different thickness around DNA under hydration $\Gamma = 11$ corresponding to the percolation threshold.[22] The power law distribution expected at the percolation threshold is shown by straight lines. For clarity, the distributions are shifted consecutively along the Y-axis by 1 order of magnitude each, starting from the bottom.

long-range diffusion this difference disappears apparently because the effect of confinement is stronger in the A-DNA shell. For ions a similar relationship holds only with small Γ. The ion mobility near B-DNA rapidly grows with hydration and eventually exceeds that for A-DNA. Interestingly, the crossover occurs with $\Gamma \approx \Gamma_t$.

The differences in the dynamics of the A- and B-DNA hydration shells revealed in Figure 6 are due to their distinct structures. Under low hydration, water and ions leave the shallow minor groove of A-DNA, but the deep major groove remains filled and the water HB network here partially retains a 3D character. As a result, water molecules in low hydration A-DNA shells have a larger number of hydrogen-bonded neighbors compared to B-DNA (see Figure 7 of ref 22), which explains the effect displayed in the left panel of Figure 6 because the mobility of hydration water near biomolecular surfaces commonly grows with the average number of water−water hydrogen bonds.[47] With hydration increased, water gradually fills the minor A-DNA groove where the percolation transition eventually occurs.[22] The minor groove water has the average number of hydrogen-bonded neighbors typical for 2D HB networks; therefore, beyond the percolation threshold the relative contribution of the fast 3D water progressively decreases. The concerted inflection of all the $D_\tau(\Gamma)$ plots with $\Gamma \approx \Gamma_t$ revealed in Figure 6 is probably due to the above scenario. The percolation transition cannot directly affect the mobility of ions because almost all of them stay in the major A-DNA groove even under the highest hydration studied. The rare events when some ions temporarily populate the minor groove are probably responsible for the increased noise observed with $\Gamma > \Gamma_t$ in Figure 6 for the long-range ion diffusivity.

Since the A-DNA form is significantly populated for $\Gamma < 15$ it could, in principle, be involved in the first stepwise increase of the conductivity of DNA fibers observed in experiment at $\Gamma \approx 15$.[39,40] However, the results shown in Figure 6 indicate that the changes in the A-DNA hydration shell hardly contribute to this effect. The ion mobility can drastically increase only in the course of the conformational switch from A- to B-DNA with $\Gamma > 15$ due to the acceleration effect of the spanning HB network around B-DNA. Therefore below we focus our attention exclusively upon the B-DNA hydration shell.

3.2. Thickness of B-DNA Hydration Shell. Earlier we showed that the water percolation transition takes place in this system with the transition midpoint at $\Gamma_m \approx 14.3$.[21,22] The first of the three steps revealed in Figure 5 exactly coincides with the midpoint of the percolation transition. This hydration level remarkably agrees with the experimental midpoint of the transition between A- and B-DNA forms and also with the onset of the experimental conductivity in DNA fibers.[40] The experimental DNA conductivity exhibits another stepwise increase at hydration $\Gamma \geq 20$.[40] For a better understanding of the origin of the two steps in Figure 5 at $\Gamma \approx 18.5$ and 23.5 and their possible relation to the experimental DNA conductivity, we carried out a detailed analysis of the changes in the water structure in the DNA hydration shell.

Under hydrations beyond the percolation threshold, 2D hydration shells can be characterized by the minimal width L_m of the surface layer where the HB water network already exhibits the spanning property. When water is adsorbed at a hydrophilic surface it forms a monolayer, and the percolation transition occurs within this narrow shell. Earlier studies showed that, in agreement with this scenario, the L_m value for protein surfaces under infinite hydration is about 4.6 Å at $T = 300$ K.[36] Figure 7 estimates L_m for DNA hydration at $\Gamma = 16$, which is just near the percolation threshold. Surprisingly, under these conditions water in narrow surface layers is still dispersed in small clusters and the spanning property appears only if the boundary is shifted to 6.4 Å from the DNA. This distance corresponds to

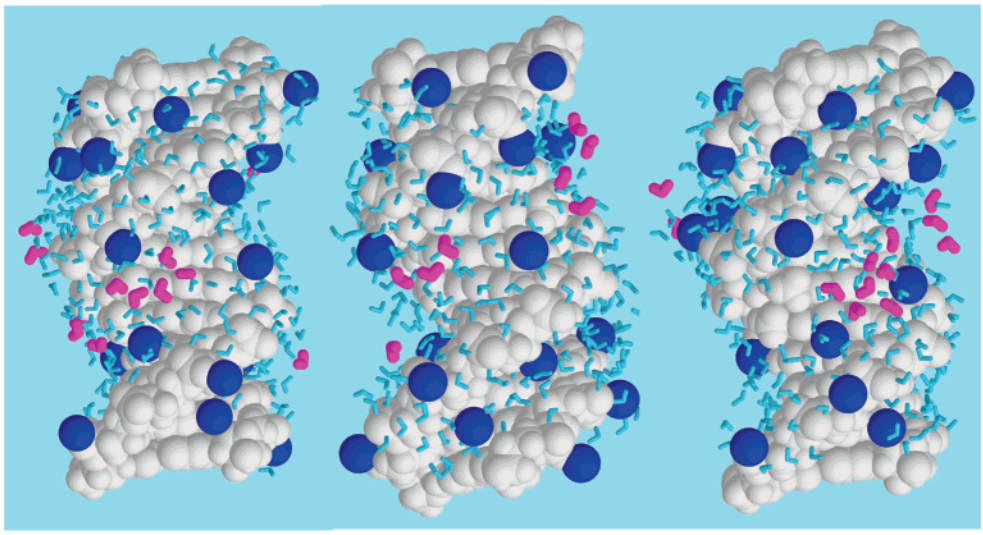

Figure 9. Three representative snapshots of the DNA hydration shell under hydration $\Gamma = 16$. Only water molecules forming the largest spanning cluster are displayed. The corresponding states were selected to have more than 85% of all water molecules involved in the largest cluster. Sodium ions are shown as blue van der Waals spheres. Water molecules at distances larger than 6 Å from the DNA surface are highlighted.

the usual thickness of two water layers[36] whereas the amount of water available at hydration $\Gamma = 16$ is largely insufficient even for one complete coverage. One can suggest that the second water layer starts to form before the first one is completed and that the spanning HB network is formed by using water molecules from this second layer. Another possibility is that the water molecules at 6.4 Å from the DNA surface actually belong to the coordination shells of Na^+ ions stuck to DNA and that the first water layer covers the DNA together with ions. To check the second possibility a similar analysis was carried out for ion-free hydration shells of uniformly neutralized B-DNA. The percolation threshold in this system was earlier localized at $\Gamma_t \approx 11$.[22] Figure 8 shows that in this case the apparent thickness of the water shell at the percolation threshold is indeed reduced compared to Figure 7. The spanning properties evaluated by the cluster size distribution n_S noticeably worsen when the thickness of the water layer is reduced to about 4.6−4.7 Å which is comparable with the value 4.6 Å obtained at the same temperature for water percolation at protein surfaces.[36]

Figure 9 shows three representative snapshots of the spanning water clusters formed at the B-DNA surface in the presence of Na^+ ions. Each of these three clusters involves more than 85% of all water molecules. The members of the spanning cluster at distances larger than 6 Å from the DNA surface are highlighted. It is seen that ions really stay adhered to DNA and that the spanning HB network sometimes covers them by using outer water molecules. Such cases are rare, however, and most often the distant members of the spanning clusters are found in the opening of the major groove. This water does not really form a second layer; rather the hydration shell as a whole looks very friable, and the HB water network bridges across the grooves although the major groove is not yet filled and there are large zones where the first water layer is not yet formed. This behavior is probably due to the strong electrostatic field around DNA.

With Γ increased, the hydration shell gradually transforms to its state in solution and L_m is expected to approach the width of one water layer. By definition, the probability R to find a spanning cluster equals 50% in the midpoint of the percolation

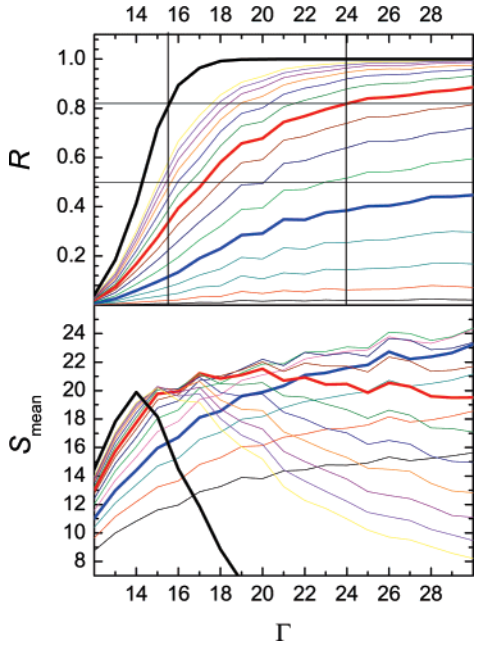

Figure 10. Hydrated DNA with ions. Probability R to find a spanning water cluster (upper panel) and the mean size of finite water clusters S_{mean} (lower panel) within the hydration layer of width L (from 4.3 to 5.7 Å with a step of 0.1 Å). Horizontal lines marked at $R = 0.50$ and 0.82 indicate the midpoint and the true threshold of the percolation transition, respectively. Thick black, red, and blue lines correspond to $L = \infty$, 5.1 Å, and 4.7 Å, respectively.

transition. At the true percolation threshold, R is usually higher, and for the present system it is about 82%. The upper panel of Figure 10 shows that, in narrow layers with $d \leq 4.7$ Å, the probability of formation of a spanning water network does not reach 50% even under full hydration. The minimal width of a water layer in which the percolation threshold is reached is about 5.1 Å. This is evidenced by the dependence $S_{mean}(\Gamma)$, shown in the lower plate of Figure 10. Only for $L > 5.1$ Å it shows a maximum characteristic for the percolation transition. The true percolation threshold is most accurately located by comparing the shape of the cluster size distribution n_S with the universal power law. Figure 11 shows that with $\Gamma \geq 24$ the n_S distributions

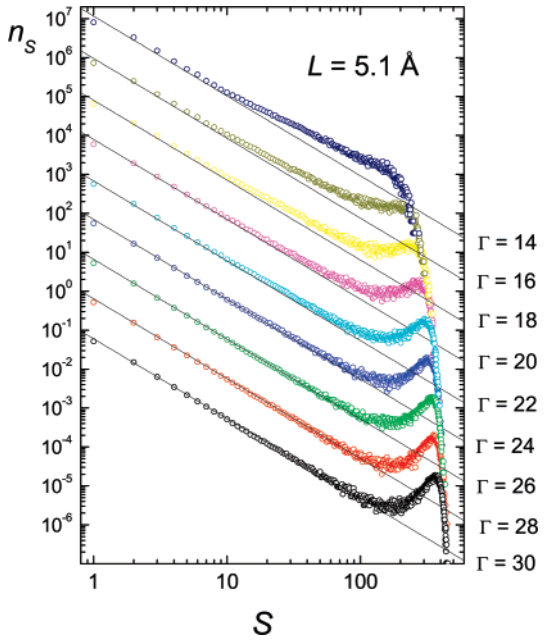

Figure 11. Hydrated DNA with ions. Probability n_S to find a water cluster of size S in the hydration shell of the width $L = 5.1$ Å at several hydrations Γ indicated in the figure. The power law distribution expected at the percolation threshold is shown by straight lines. For clarity, the distributions are shifted consecutively along the Y-axis by 1 order of magnitude each, starting from the bottom.

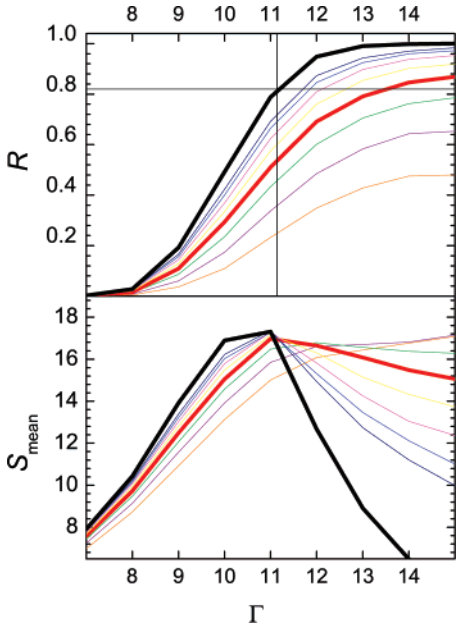

Figure 12. Hydrated DNA without ions. Probability R to find a spanning water cluster (upper panel) and the mean size of finite water clusters S_{mean} (lower panel) within the hydration shell of width L (from 4.3 to 5.0 Å with a step of 0.1 Å). The horizontal line at $R = 0.82$ indicates the true percolation threshold. Thick black and red lines correspond to $L = \infty$ and 4.6 Å, respectively

in 5.1 Å water layers follow the critical power law in the widest range of cluster sizes and that deviations from this law appear under lower hydrations. Therefore, the limiting L_m value is about 5.1 Å, which is much larger than 4.6 Å observed for proteins.[36] The difference may be due to a high concentration of ions in the DNA hydration shell in the considered hydration range.

Analysis of ion-free hydration shells of uniformly neutralized DNA partially confirms this explanation. Figure 12 shows that without ions the narrowest layer where the true percolation threshold is reached is about 4.6, i.e., the same as that for protein surfaces. The above estimates are additionally supported by the number of H-bonded water neighbors in various hydration shells (Figure 13). As expected, both with and without ions the hydration shells at the percolation threshold are characterized by the average number n_H of hydrogen bonds per water molecule close to 2.0.[55] Note that in the presence of ions the n_H values appear slightly lower, which should be attributed to "roughening" of the DNA surface since the critical value of n_H is lower in 3D than in 2D systems.[58]

3.3. Radial Ion Distributions. Additional information about the interplay between water structure and ion mobility may be extracted from the evolution of ion distributions around DNA. Earlier analysis shows that the B-DNA surface is very nonuniform.[22] Although the minor groove hydration shell under low hydration looses some water from outer layers, it remains filled and the solvation conditions of surface atoms as well as ions change very little. In contrast, the major groove hydration shell evolves, and here the spanning HB water network is reversibly broken and formed via a percolation transition. Figure 14 shows how these changes reflect upon the surface radial distribution functions of Na^+ ions. Under the highest hydration used, the radial distribution function involves three peaks centered at 2.5, 4.2, and 6.5 Å, respectively (Figure 14a). The first peak corresponds to Na^+ ions bound to negatively charged DNA atoms by strong electrostatic forces. The second peak corresponds to van der Waals contacts of Na^+ ions with neutral or weakly charged DNA atoms. The third broad peak appears under high hydrations and corresponds to fully hydrated Na^+ ions separated from DNA by a water molecule. Under low hydration, ions are stuck to DNA and Figure 14a suggests that with $\Gamma < 12$ they all eventually form ion pairs. It is seen that the relative weight of the second peak rapidly grows with $\Gamma \geq 12$ and plateaus at about $\Gamma = 15$, that is close to the percolation threshold. One of the effects known to occur upon hydration of biosystems under low humidity consists of the rapid growth of their static dielectric constant at about monolayer water coverage.[63−65] This effect originates from the appearance of "freely" rotating water molecules and is strongly enhanced due to the formation of a cooperative HB water network at the percolation threshold.[47,65]

The drastic change in the ion radial distributions seen in Figure 14b between $\Gamma = 12$ and 15 features the dissociation of ion pairs due to an increased water dielectric constant and explains the stepwise increase of the long-range ion mobility at $\Gamma = 14.5$ in Figure 5. Comparison of Figures 5 and 14b reveals that the growth of the relative weight of the third peak of radial distributions shown in Figure 14a essentially repeats that of the long-range ion mobility. Unlike ions blocked in the first DNA hydration layer, fully hydrated ions can cover long distances and make a dominant contribution to the average long-range ion mobility.

Figure 15 shows how the minimal thickness of the spanning water shell L_m changes with hydration. This figure summarizes the effects discussed in the previous section and displayed in

(63) Rosen, D. *Trans. Faraday Soc.* **1963**, *59*, 2178−2191.
(64) Tomaselli, V. P.; Shamos, M. H. *Biopolymers* **1973**, *12*, 353−366.
(65) Bone, S.; Pethig, R. *J. Mol. Biol.* **1982**, *157*, 571−575.

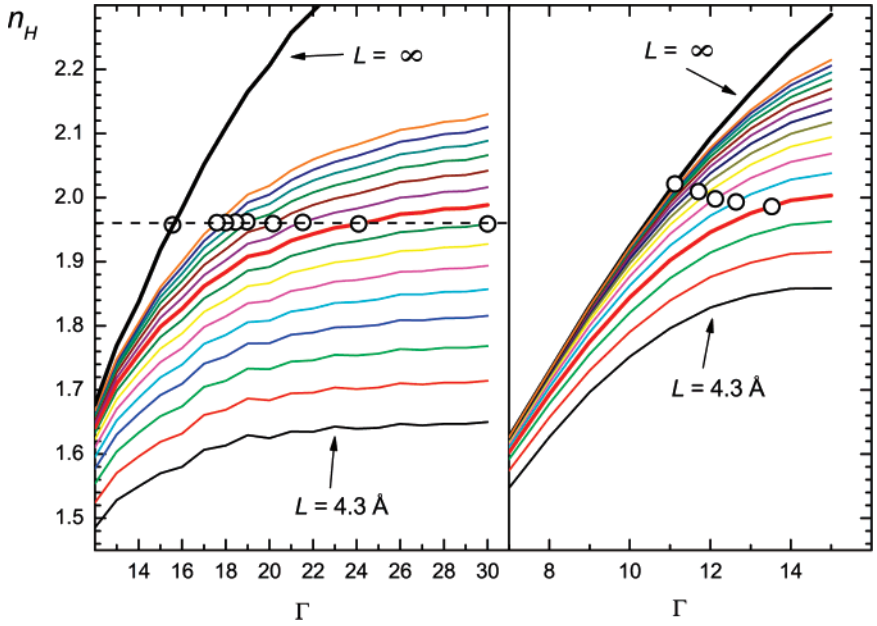

Figure 13. Average number n_H of hydrogen-bonded neighbors per a water molecule within hydration shells of different width L (from 4.3 to 5.7 Å with a step of 0.1 Å). DNA with ions (left panel) and uniformly neutralized DNA without ions (right panel). Thick red lines correspond to $L = 5.1$ and 4.6 Å on the left and right panels, respectively. True percolation thresholds are marked by open circles. The horizontal line indicates the value $n_H = 1.96$.

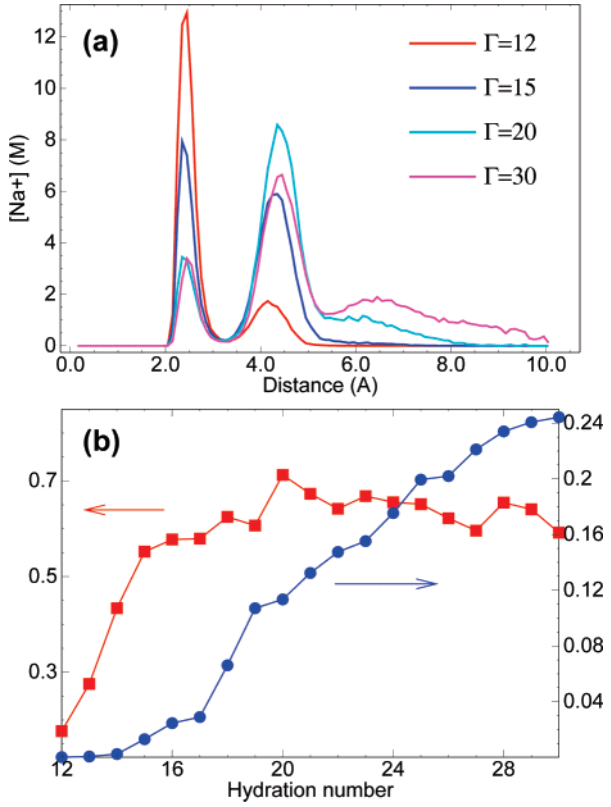

Figure 14. (a) Surface radial distribution functions of Na^+ ions under a few representative hydration numbers indicated in the figure. Absolute ion concentrations are shown. (b) Evolution of ion distributions with hydration. The relative weights corrected for the volume increase were measured for the second (red squares) and third (blue circles) peaks in the distributions shown in plate (a).

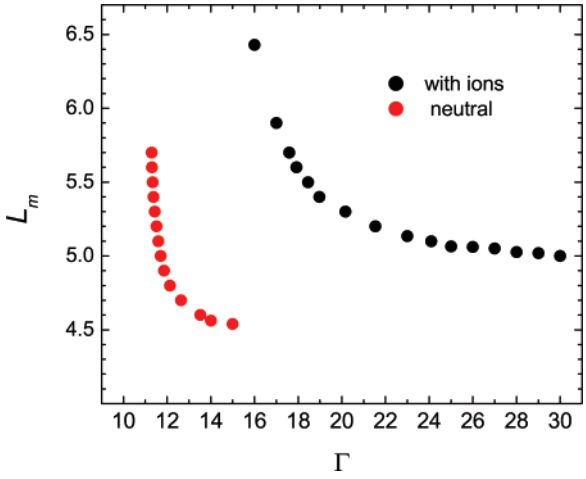

Figure 15. Thickness L_m of the minimal percolating water layer around DNA under different hydrations.

Figures 10−12. Comparison of Figures 14 and 15 indicates that the stepwise increase in the long-range ion mobiltiy at $\Gamma = 18.5$ (Figure 5) and the corresponding drastic increase in the relative fraction of fully hydrated ions (Figure 14b) occur with $L_m \approx 5.5$ Å, which is exactly the border between the second and the third peaks in Figure 14a. At this hydration the spanning HB network is formed in the 5.5 Å water layer, which facilitates detachment of ions from the DNA surface. The smaller stepwise increase in ion mobility seen in Figure 5 at $\Gamma = 23.5$ may have a similar origin. Under this hydration Na^+ ions appear at distances beyond 8 Å from the DNA surface, seen as a tail in the radial distribution function for $\Gamma = 30$ in Figure 14a. These ions are separated from the DNA surface by two water layers, and they are yet more mobile.

Discussion

The results presented here reveal an intricate interplay between ion dynamics and the state of hydration water at the DNA surface under low humidity. The percolation transition and formation of spanning HB water networks around DNA are shown to play a major role. This factor ealier was paid little attention. A quantitative analysis of water and ion dynamics in this system is complicated by the existence of natural boundaries. Both water and ion diffusion accelerate with hydration.

For water, this acceleration is qualitatively and quantitatively similar on all length scales studied. A curious linear correlation is observed between the rate of water diffusion and the average size of the maximal water cluster in the hydration shell. The acceleration of ion diffusion with hydration is nearly linear for short-range translations, but the long-range ion diffusivity additionally involves stepwise acceleration at distinct hydration numbers. Additional studies are necessary in order to rationalize all the mechanisms involved in these effects. The overall acceleration of diffusion with increased hydration is not trivial; notably, its origin may differ for water and ions. In the present study we focused upon the stepwise increase of the long-range ion diffusivity at certain degrees of hydration.

The first drastic increase in the long-range ion mobility occurs within the hydration range Γ from 13 to 16 (see Figure 5) just around the midpoint of the B- to A-DNA transformation.[39,40] It closely follows the spanning probability of the percolation transition of water in the hydration shell[21] (see the thick black line in the upper panel of Figure 10) and the sigmoidal increase in conductivity of DNA fibers.[40] All these observations concertedly point at the key role of ion dynamics and water percolation in the molecular mechanism of A/B polymorphism in DNA. Here we have found additionally that the acceleration of ion diffusion coincides with dissociation of ion pairs at the DNA surface suggesting that the water percolation transition is accompanied by a drastic increase in the dielectric permittivity of the hydration shell. The relationship between water percolation and the static dielectric permittivity is physically reasonable. Rapid growth of the static dielectric constant upon hydration was observed experimentally in different biosystems at about a monolayer water coverage.[63−65] The first appearance of such a monolayer usually occurs via a percolation transition of hydration water.[32,35,55] A direct relationship between water percolation and the drastic increase of the dielectric permittivity is supported by experimental studies of lysozyme powder where the percolation transition of water was accurately located at about 0.140 g/g (g of water per gram of protein),[27] whereas the onset of a superlinear increase of the dielectric permittivity was independently detected at about 0.125 g/g.[65]

The dielectric permittivity of a tiny water shell cannot be easily measured in simulations, and its possible change with hydration was not earlier considered in the context of polymorphic transitions in DNA. This newly uncovered effect is important because it brings a missing link between water percolation and the electrostatic condensation mechanism of B- to A-DNA transitions under low humidity. All earlier experimental and computational observations agree with the following scenario of A $\leftrightarrow$ B transitions.[19−21] When B-DNA hydration is reduced, and the H-bonded water network approaches the percolation threshold, free sodium ions lose translational entropy and tend to accumulate in the major groove. This increases the electrostatic tension across the major groove and eventually leads to intraduplex electrostatic condensation that pushes DNA from the B- to A-form. The stepwise character of this transition was always thought to be due to the intrinsic structural cooperativity involved in the A $\leftrightarrow$ B transformation.[19,66] Its closeness of the water percolation threshold was attributed to the lower conformational energy of the B-DNA conformation so that transitions to the A-form start only when the spanning H-bonded water network approaches its limit.[22] The foregoing pattern remains entirely valid. Our present study suggests additionally that the electrostatic condensation is probably provoked by a dramatic decrease of the static dielectric permittivity upon breakage of the spanning water HB network.

With hydration increased beyond the percolation transition the water shell around DNA continues to evolve. We were surprised to find out that the first spanning HB network formed at the percolation threshold is unusually thick and friable compared to earlier studied protein hydration shells. This effect is due to the strong electrostatic field around DNA, and it is modulated by the presence of ions. Stable water layers transpierced by a spanning HB network are formed with significantly higher hydrations. Analysis of water percolation in zones of different widths around DNA is a useful tool that helps to reveal qualitative changes in the DNA hydration shell with increased amounts of water molecules. Our results suggest that in the presence of Na^+ ions the minimal thickness of the percolating water layer around DNA does not decrease below $L_m \approx 5.1$ Å in the considered range of hydrations (Figure 15). This is mainly due to a significant ion concentration in the first DNA hydration layer. Without ions the L_m value falls to approximately 4.6 Å, which is similar to that for protein surfaces under the same temperature.[36]

The two stepwise increments in the long-range ion mobility observed with $\Gamma = 18.5$ and 23.5 correlate with formation of consecutive percolating water layers on the DNA surface acompanied by the progressive escape of sodium ions into solution. In experiment, only one additional drastic increase of conductivity of DNA samples is observed under hydrations $\Gamma \geq 20$.[40] Its origin was attributed to the appearance of fully hydrated ions with bulklike mobility. We suppose that this experimental observation corresponds to the increase of ion mobility at hydration $\Gamma = 18.5$ in our simulations; i.e., it is due to ions separated from DNA surfaces by one water layer. The small discrepancy in the hydration numbers can be due to intermolecular contacts and higher ion concentrations in DNA fibers. Additional stepwise increments in conductivity at higher hydrations probably could not be resolved in experiments.

A number of aspects of ion involvement in DNA hydration remain controversial and require additional studies. The present findings partially explain why not only the B to A transition but also a variety of very different transformations are observed in B-DNA under hydration $\Gamma \leq 20$. It is long known, for instance, that Li-DNA cannot adopt the A-form; however, it does not stay in the B-form and switches to the C-form instead.[9,48,66,67] The B to C transition also occurs in Na-DNA fibers subjected to an external stretching force.[68] Both B $\leftrightarrow$ A and B $\leftrightarrow$ C transformations are observed in a narrow range of hydrations about $\Gamma \leq 20$ suggesting that they are driven by the same physical forces; however, these driving forces should not depend upon the DNA conformation because the C-form

(66) Ivanov, V. I.; Minchenkova, L. E.; Minyat, E. E.; Frank-Kametetskii, M. D.; Schyolkina, A. K. *J. Mol. Biol.* **1974**, *87*, 817−833.
(67) Lee, S. A.; Lindsay, S. M.; Powell, J. W.; Weidlich, T.; Tao, N. J.; Lewen, G. D. *Biopolymers* **1987**, *26*, 1637−65.
(68) Fornells, M.; Campos, J. L.; Subirana, J. A. *J. Mol. Biol.* **1983**, *166*, 249−252.

structure is very dissimilar from the A-form.[69] Now we can reasonably assume that all these conformational transitions occur due to electrostatic condensation provoked by a drastic reduction of the static dielectric permittivity of hydration water. The specific transition pathways depend upon the DNA sequence, the type of counterions, and other conditions. Several pathways are possible because the condensation can occur in the major or minor DNA grooves, or else between the neighboring duplexes in a condensed phase. Some of the above scenarios can be probed by MD simulations, and these studies are now in progress.

Acknowledgment. I.B., A.K., and A.O. thank DFG (Forschergruppe 436) for financial support.

JA0732882

(69) van Dam, L.; Levitt, M. H. *J. Mol. Biol.* **2000**, *304*, 541−561.